Multispectral MRI Centerline Tracking in Carotid Arteries

Hui Tang[a,d], Theo van Walsum[a], Robbert S. van Onkelen[b,c], Stefan Klein[a], Reinhard Hameeteman[a], Michiel Schaap[a], Quirijn J.A. van den Bouwhuijsen[b,c], Jacqueline C. M. Witteman[c], Aad van der Lugt[b], Lucas J. van Vliet[d], Wiro J. Niessen[a,d]

[a]Department of Medical Infomatics
[b]Department of Radiology
[c]Department of Epidemiology
Erasmus MC-University Medical Center Rotterdam, The Netherlands
[d]Department of Imaging Science and Technology, Faculty of Applied Science
Delft University of Technology, The Netherlands

ABSTRACT

We propose a minimum cost path approach to track the centerlines of the internal and external carotid arteries in multispectral MR data. User interaction is limited to the annotation of three seed points. The cost image is based on both a measure of vessel medialness and lumen intensity similarity in two MRA image sequences: Black Blood MRA and Phase Contrast MRA. After intensity inhomogeneity correction and noise reduction, the two images are aligned using affine registration. The two parameters that control the contrast of the cost image were determined in an optimization experiment on 40 training datasets. Experiments on the training datasets also showed that a cost image composed of a combination of gradient-based medialness and lumen intensity similarity increases the tracking accuracy compared to using only one of the constituents. Furthermore, centerline tracking using both MRA sequences outperformed tracking using only one of these MRA images. An independent test set of 152 images from 38 patients served to validate the technique. The centerlines of 148 images were successfully extracted using the parameters optimized on the training sets. The average mean distance to the reference standard, manually annotated centerlines, was 0.98 *mm*, which is comparable to the in-plane resolution. This indicates that the proposed method has a high potential to replace the manual centerline annotation.

Keywords: Minimum cost path, medialness, lumen intensity similarity, multispectral MRA, carotid artery, centerlines

1. INTRODUCTION

Atherosclerosis is a major cardiovascular disease.[1] MR imaging is a non-invasive technique to assess atherosclerotic plaque volume and composition and to monitor plaque progression. (Semi-)automated processing of these images is valuable, both in clinical practice and in clinical research. Consequently, vascular image processing has been an important topic in the field of medical imaging.[2] In many vascular image processing algorithms, centerlines either serve as the initialization for segmentation,[3–5] or define the region of interest for further processing.[6] The purpose of this research is to develop and evaluate an algorithm for (semi-)automatic centerline extraction in carotid MR images with minimal user interaction. Many centerline tracking algorithms are based on a minimum cost path approach. The centerline is the path with minimum accumulative cost between two given points, determined e.g. via a graph-based search technique,[7] or a levelset based approach.[8] The most important factor in these methods is the cost image, which must have low values at the vessel center and high values at other locations. Many ways to construct a cost image from the input data have been proposed. They are usually based on intensity, gradient and second order information[9,10] to get a high response in the middle of the lumen. So far these centerline tracking methods are based on only one scan and evaluated on a small number of datasets. In this paper, a minimum cost path based approach is proposed to extract the centerlines from multispectral MRA data, consisting of both Black Blood MRA (BBMRA) and Phase Contrast MRA (PCMRA). The main contribution of this paper is twofold. First, the cost image is based on the information from two

---

Email: h.tang@tudelft.nl

(a) original BBMRA   (b) unbiased BBMRA   (c) denoised BBMRA

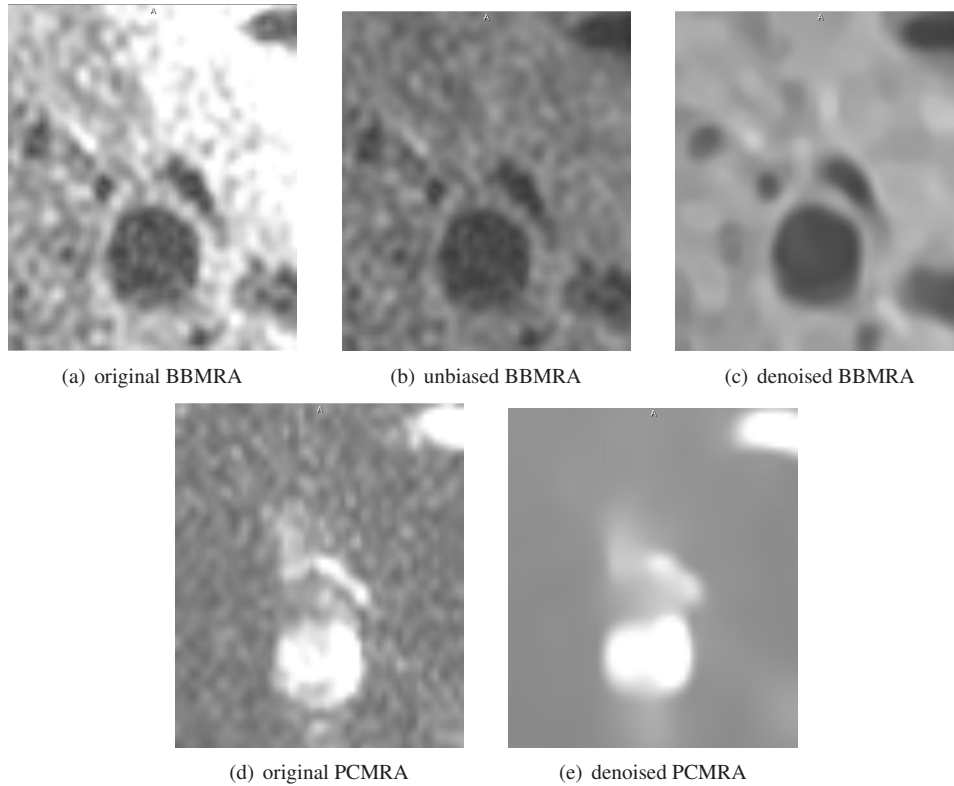(d) original PCMRA   (e) denoised PCMRA

Figure 1. An example of the original and preprocessed images

different MRA sequences instead of only one sequence. Second, the proposed method is evaluated on a large number of datasets with varying image qualities.

The rest of this paper is organized as follows. Section 2 presents the method. Section 3 discusses the parameter optimization on 40 training data sets and shows the experimental results on 152 testing data sets. A discussion and conclusions is given in section 4.

2. METHODS

2.1 Preprocessing

To correct for intensity inhomogeneity that commonly affects MR images, we applied the N3 bias correction method[11] implemented by Tustison et al.[12] to all BBMRA images as a preprocessing step. This step was not performed on PCMRA, since these images suffer less from intensity inhomogeneities. Both images were subsequently denoised via edge enhancing diffusion to preserve the edges around the lumen.[13] After bias correction and denoising, the BBMRA and PCMRA datasets were aligned by an affine registration using Elastix,[14] a publicly available software tool that allows intensity based image registration. Fig.1(a) to Fig.1(e)show an example of the original and preprocessed MRA images. The preprocessed images are used in all experiments.

2.2 Minimum cost path between seed points

In the minimum cost path approach, we aim to find the path with minimal accumulated cost $E(\boldsymbol{C})$ between the start and end seed points.[15] The accumulated cost $E(\boldsymbol{C})$is defined as:

$$E(\boldsymbol{C}) = \int_{s_1}^{s_2} P(\boldsymbol{C}(s))|\boldsymbol{C}'(s)|ds \qquad (1)$$

where $P(\boldsymbol{x})$ is the so called potential or cost at location $\boldsymbol{x}$, and s denotes the parameterization of the path $\boldsymbol{C}$. The costs $P(\boldsymbol{x})$ should be small in the center of the vessel and large in all other areas. The object is to find curve $\boldsymbol{C}$ which minimizes Eq.1. This so-called *shortest path* is determined by applying Dijkstra's algorithm in a 26-connected neighborhood[7] simultaneously to the selected seed points.

2.3 Cost function definition

2.3.1 Medialness

We use a measure for medialness[16] for constructing the cost image, see Fig.2(a) and Fig.2(b). We chose Gülsün's definition of medialness instead of the one based on the well-known Hessian matrix,[9,10] as the latter was demonstrated to fail in enhancing vessel bifurcations.[16] Note that in this paper, the medialness is calculated in the direction of the z coordinate, as generally the carotid artery runs approximately perpendicular to the lateral slices except in the bifurcation area. The medialness is a normalized value between 0 and 1 and is determined for both the BBMRA ($m_{BB}(\boldsymbol{x})$) and the PCMRA ($m_{PC}(\boldsymbol{x})$) scans. Very weak image contrast results in a low medialness value, which may hamper the centerline tracking. We assume that the images with the highest contrast produce more reliable information. Hence a combined multispectral medialness can be obtained by taking the maximum of both values:

$$m_{BBPC}(\boldsymbol{x}) = max(m_{BB}(\boldsymbol{x}), m_{PC}(\boldsymbol{x})) \tag{2}$$

2.3.2 Lumen intensity similarity

To prevent the centerline from taking a shortcut through the background, the cost image can be improved by adding a lumen intensity similarity term, which increases the costs in the background. Since the intensity in the lumen is suppressed for BBMRA but enhanced for PCMRA, the lumen intensity similarity is defined differently for BBMRA($s_{BB}(\boldsymbol{x})$)) and PCMRA ($s_{PC}(\boldsymbol{x})$))

$$s_{BB}(\boldsymbol{x}) = \begin{cases} exp(-(\frac{I_{BB}(\boldsymbol{x})-\mu_{BB}}{\sqrt{2}\sigma_{BB}})^2), I_{BB}(\boldsymbol{x}) > \mu_{BB} \\ 1, I_{BB}(\boldsymbol{x}) <= \mu_{BB} \end{cases} \tag{3}$$

$$s_{PC}(\boldsymbol{x}) = \begin{cases} exp(-(\frac{I_{PC}(\boldsymbol{x})-\mu_{PC}}{\sqrt{2}\sigma_{PC}})^2), I_{PC}(\boldsymbol{x}) < \mu_{PC} \\ 1, I_{PC}(\boldsymbol{x}) >= \mu_{PC} \end{cases} \tag{4}$$

where $I(\boldsymbol{x})$ is the intensity at position $\boldsymbol{x}$. The mean μ and standard deviation σ of the lumen intensity distributions are estimated from the intensities in a small, spherical region around each of the manually provided seed points. The sphere radius was set to be 2.5 *mm* for the seed point in the common carotid and 1.5 *mm* in the internal or the external carotid artery. These values are large enough to obtain reliable statistics, but sufficiently small to exclude background values. Similar to the definition of combined medialness, we expect high lumen intensity similarity in the lumen area. Hence, the multispectral lumen intensity similarity is defined as the voxelwise maximum of the two lumen intensity similarities.

$$s_{BBPC}(\boldsymbol{x}) = max(s_{BB}(\boldsymbol{x}), s_{PC}(\boldsymbol{x})) \tag{5}$$

2.3.3 Cost definition

The medialness and the lumen intensity similarity terms are high in the center of the vessel and low elsewhere. We propose the following cost function that is inversely proportional to the product of two measures:

$$P(\boldsymbol{x}) = \frac{1}{\epsilon + m_{BBPC}(\boldsymbol{x})^\alpha s_{BBPC}(\boldsymbol{x})^\beta} \tag{6}$$

in which ϵ is a small positive value to avoid division by zero (ϵ is set to 1e-6), α and β are two positive weighting parameters to control the contrast of the cost image. If the cost only includes medialness, β is set to be zero. Fig.2(a) to Fig.2(f)show an example of the medialness and lumen intensity similarity in monospectral and multispectral scans. It can be seen that artifacts in either of the two scans are compensated in the combined lumen intensity similarity image.
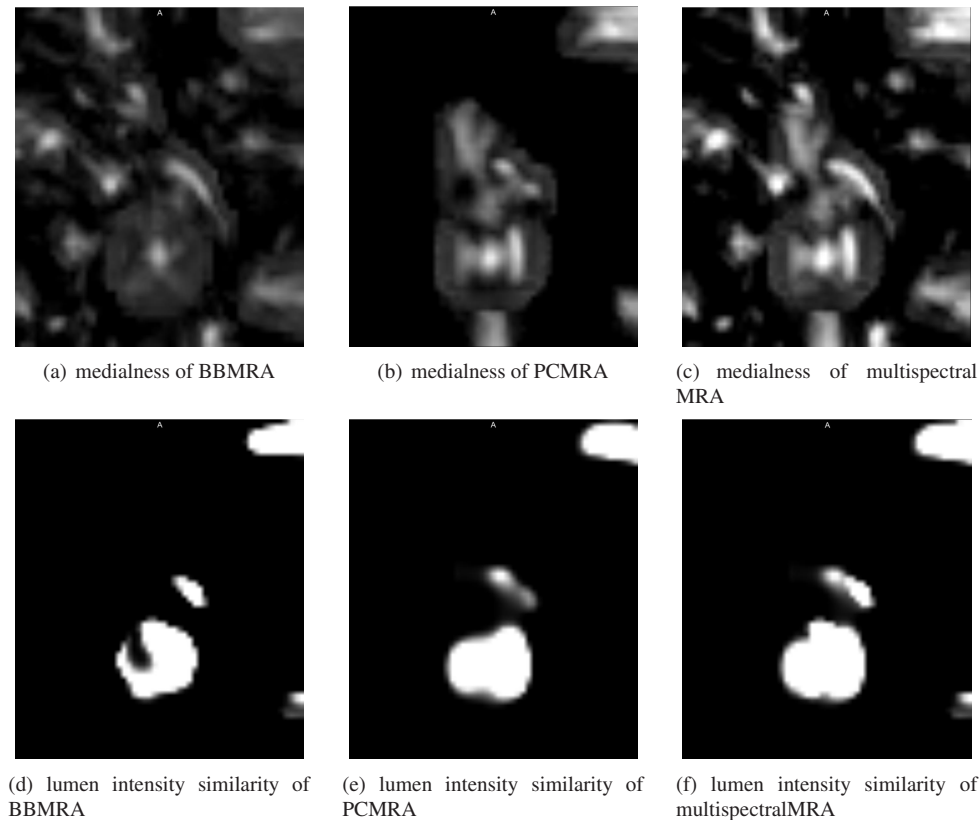
(a) medialness of BBMRA   (b) medialness of PCMRA   (c) medialness of multispectral MRA

(d) lumen intensity similarity of BBMRA   (e) lumen intensity similarity of PCMRA   (f) lumen intensity similarity of multispectralMRA

Figure 2. An example of the items for cost definition

# 3. EXPERIMENTS AND RESULTS

3.1 Image data and reference standard

The proposed method was applied to both carotid arteries of 48 subjects, who were scanned twice within a short period (time between scans is 15±9 days), resulting in a total of 192 carotid arteries. The BBMRA images were acquired with a field-of-view (FOV) of 13×13 cm^2, a matrix of 160×128 pixels, an in-plane resolution of $0.8 \times 1mm^2$ before interpolation and 0.5×0.5 mm^2 after interpolation, and a 0.90 *mm* slice thickness. The PCMRA images had a FOV of 18×18 cm^2, a matrix of 256×128 pixels, an in-plane resolution of 0.7×1.4 mm^2 before interpolation and 0.7×0.7 mm^2 after interpolation, and a 1.0 *mm* slice thickness. For each carotid artery a centerline was delineated by an experienced observer in the BBMRA data using in-house developed software.[17] The annotated centerlines were used as the reference standard for the parameter optimization and evaluation of the accuracy of the proposed tracking approach. Parameter optimization was performed on 40 arteries from 20 representative scans (i.e. 10 patients) that were selected as training datasets. The remaining 152 arteries from 38 patients were used for testing. For all of the arteries, the beginning and end points of the manual centerlines are used as the start and end points for the automated method, which means that the centerline is tracked in the same region as selected by observers.

3.2 Parameter optimization

All parameters for bias field correction were set to the author-suggested parameter values.[12] The parameters for the edge enhancing diffusion were optimized by visual inspection of the training datasets and were chosen as follows: The Gaussian at which the gradient was calculated was set to 1.0 *mm*, and 10 iterations with a time step of 0.15 were used in the anisotropic diffusion. For the medialness calculation we used a gradient scale of 1.0 *mm* for both BBMRA and PCMRA as the two scans have a low in-plane resolution, a maximum radius of 15.0 *mm*, and 24 angles. The training datasets were used to tune the two parameters α and β, which control the cost function. Both parameters were tested in the interval from 1 to 4 with a step size of 1, leading to 16 possible combinations. We compared the

Table 1. optimization of α and β in centerline tracking

Images	cost Image	min # of failures	max # of failures	mean distance(mm)	α	β
BBMRA	medianess	7	10	0.96	3	0
	medialness+lumenSimilarity	3	5	0.90	2	1
PCMRA	medianess	5	6	1.16	2	0
	medialness+lumen similarity	2	3	1.12	1	1
multispectral	medianess	2	5	1.04	2	0
	medialness+lumenSimilarity	0	0	1.08	1	1
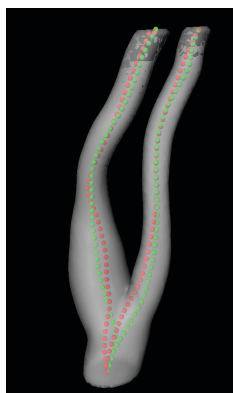
(a) An example of the tracked centerline(Mean distance=0.93mm)
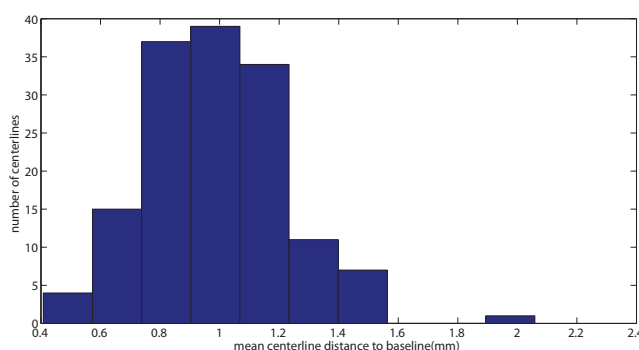
(b) mean distance distribution of 148 centerlines(mm)

Figure 3. An example of a tracked centerline with the average mean distance and the accuracy distribution of the 148 centerlines

performance obtained by all 16 combinations of cost images for all images in the training set. As our focus is on automated processing, the main evaluation criterion is the number of successfully extracted centerlines. If the number of error centerlines is zero, we chose the smaller α and β. In our case, unsuccessful extractions included: (1) leakage into a non-carotid artery, or (2) leakage from the external carotid to the internal carotid or vice versa. Unsuccessful extraction was determined by visual inspection. For the successfully extracted centerlines, we also calculated the average distance to the manually obtained reference standard. We use the average centerline distance[3] to quantify the accuracy of the tracked centerline.

Tab.1 lists the minimum and maximum number of failed centerline extractions over all combinations of α and β for each of the cost image combinations(only BBMRA, only PCMRA, Multispectral MRA). The average centerline distance is listed for all successfully extracted centerlines as well as the optimal setting for α and β. It shows that the number of failed centerline extractions is reduced by adding the intensity similarity term to both the monospectral and the multispectral centerline tracking. This indicates that multispectral centerline tracking is more robust than monospectral centerline tracking. All centerlines were found using the multispectral approach employing the two-term cost image for the optimal setting of $\alpha = \beta =1$, which demonstrates the method's robustness with respect to the parameters α and β. The slightly better accuracy of the centerlines extracted from the BBMRA images alone may be caused by a residual registration error, as the centerlines were annotated on the BBMRA images.

3.3 Quantitative evaluation on large datasets

The method with its optimized parameters, using multispectral data and $\alpha=\beta=1$, has been applied to the entire test set and successfully extracted 148 out of the 152 centerlines with an average mean distance of 0.98 mm to the reference standard for the successfully extracted centerlines. A tracked centerline (red) with an average mean distance (0.93mm) to the manually annotated reference standard (green) is shown in Fig.3(a), surrounded by the transparent lumen. The accuracy distribution of all the centerlines is shown in Fig.3(b).

4. DISCUSSION AND CONCLUSIONS

The testing data shows that 90 out of 148 centerlines have a mean centerline distance below 1.0*mm*. The four failures were due to the highly curved vasculature; in three cases a path runs from the external to the internal carotid artery (or vice versa), and in one case the path shortcuts a very curved internal via a nearby straight vessel. The practical use of this method can be improved by adding an automatic failure detection.

We proposed a minimum cost path based method to track the centerline tree around the carotid bifurcation based on user-defined seed points. The three seed points are the begin and end points of the manual centerlines, which guarantees that the region of interest from the clinical point of view is included. The cost image for the minimum cost path algorithm combines both a gradient-based medialness and an intensity-based lumen similarity derived from both the BBMRA and PCMRA images of the carotid arteries. The two scans are aligned using affine registration. Both the medialness and the lumen similarity are calculated in the two co-registered MRA scans (BBMRA and PCMRA). The cost image is based on two scans to compensate artifacts that may exist in one of the two scans. Our experiments on the training data show that the combination of medialness and lumen intensity similarity applied to multispectral MRA data outperforms centerline tracking applied to only one of the MRA images. Incorporating both the medialness and the lumen intensity similarity terms in the cost function outperforms a cost function based on only the medialness. The two parameters that control the contrast of the cost image were optimized using the 40 training datasets. The optimized centerline tracking method has been applied to 152 carotid arteries and successfully tracked 148 centerlines. The average mean distance to the manually annotated centerlines is 0.98 *mm*, which is in the range of the in-plane resolution before interpolation. A limitation of the study is that we only compared performance with respect to a single observer. In order to determine whether this method can replace manual tracking in terms of accuracy would require a multi-observer evaluation study. However, the success rate and accuracy with respect to the single observer indicates the potential of the method. Especially for automated initialization of subsequent segmentation algorithms, the performance of the algorithm is sufficiently good.

Concluding, we presented a robust and accurate method for the extraction of carotid centerlines from multispectral MR data, that has high potential to replace the manual annotation of centerlines.

REFERENCES

[1] Ross, R., "Atherosclerosis: an inflammatory disease," *New England Journal of Medicine* **340**, 115–126 (1999).

[2] Lesage, D., Angelini, E. D., Bloch, I., and Funka-Lea, G., "A review of 3d vessel lumen segmentation techniques: Models, features and extraction schemes," *Medical Image Analysis* **13(6)**, 819–845 (2009).

[3] Schaap, M., Metz, C. T., van Walsum, T., van der Giessen, A. G., Weustink, A. C., Mollet, N. R., Bauer, C., Bogunovic, H., Castro, C., Deng, X., Dikici, E., O'Donnell, T., Frenay, M., Friman, O., Hoyos, M. H., Kitslaar, P. H., Krissian, K., Khnel, C., Luengo-Oroz, M. A., Orkisz, M., Smedby, r., Styner, M., Szymczak, A., Tek, H., Wang, C., Warfield, S. K., Zambal, S., Zhang, Y., Krestin, G. P., and Niessen, W. J., "Standardized evaluation methodology and reference database for evaluating coronary artery centerline extraction algorithms," *Medical Image Analysis* **13(5)**, 701–714 (2009).

[4] Tang, H., van Onkelen, R., van Walsum, T., Hameeteman, R., Schaap, M., Tori, F., van den Bouwhuijsen, Q., Witteman, J., van der Lugt, A., van Vliet, L., and Niessen, W., "A semi-automatic method for segmentation of the carotid bifurcation and bifurcation angle quantification on Black Blood MRA," in [*Lecture Notes in Computer Science*], Jiang, T., Navab, N., Pluim, J., and Viergever, M., eds., **6363**, 97–104, Springer Berlin / Heidelberg (2010).

[5] Ladak, H. M., Thomas, J. B., Mitchell, J. R., Rutt, B. K., and Steinman, D. A., "A semi-automatic technique for measurement of arterial wall from black blood MRI," *Medical Physics* **28(6)**, 1098–1107 (2001).

[6] Shahzad, R., Schaap, M., van Walsum, T., Klein, S., Weustink, A., van Vliet, L. J., and Niessen, W., "A patient-specific coronary density estimate," in [*Proceedings of IEEE International Symposium on Biomedical Imaging: from Nano to Macro, 2010*], 9–12 (2010).

[7] Dijkstra, E. W., "A note on two problems in connexion with graphs," *Numerische Mathematik* **1(1)**, 269–271 (1959).

[8] Sethian, J., [*Level Set Methods and Fast Marching Methods*], Cambridge University Press (1999).

[9] Frangi, A. F., Niessen, W. J., Vincken, K. L., and Viergever, M. A., "Multiscale vessel enhancement filtering," in [*Lecture Notes in Computer Science, 1998, Volume 1496/1998, 130*], (1998).

[10] Sato, Y., Nakajima, S., Atsumi, H., Koller, T., Gerig, G., Yoshida, S., and Kikinis, R., "3D multi-scale line filter for segmentation and visualization of curvilinear structures in medical images," in [*CVRMed-MRCAS'97*], Troccaz, J., Grimson, E., and Msges, R., eds., *Lecture Notes in Computer Science* **1205**, 213–222, Springer Berlin / Heidelberg (1997).

[11] Sled, J., Zijdenbos, A., and Evans, A., "A nonparametric method for automatic correction of intensity nonuniformity in MRI data," *IEEE Transactions on Medical Imaging* **17(1)**, 87–97 (1998).

[12] Tustison, N., Avants, B., Cook, P., Zheng, Y., Egan, A., Yushkevich, P., and Gee, J., "N4ITK: Improved N3 bias correction," *IEEE Transactions on Medical Imaging* **29(6)**, 1310 – 1320 (2010).

[13] Perona, P.and Malik, J., "Scale-space and edge detection using anisotropic diffusion," *IEEE Transactions on Pattern Analysis and Machine Intelligence* **12(7)**, 629–639 (1990).

[14] Klein, S., Staring, M., Murphy, K., Viergever, M., and Pluim, J., "Elastix: a toolbox for intensity-based medical image registration," *IEEE Transactions on Medical Imaging* **29**(1), 196–205 (2010).

[15] Caselles, V., Kimmel, R., and Sapiro, G., "Geodesic active contours," *International Journal of Computer Vision* **22(1)**, 61–79 (1997).

[16] Gülsün, M. A. and Tek, H., "Robust vessel tree modeling," in [*Proceedings of the 11th international conference on Medical Image Computing and Computer-Assisted Intervention - Part I*], *MICCAI '08*, 602–611, Springer-Verlag, Berlin, Heidelberg (2008).

[17] Hameeteman, K., Freiman, M., Zuluaga, M., Joskowicz, L., Rozie, S., van Gils, M., van den Borne, L., Sosna, J., Berman, P., Cohen, N., Douek, P., Sánchez, I., Aissat, M., van der Lugt, A., Krestin, G. P., Niessen, W., and van Walsum, T., "Carotid lumen segmentation and stenosis grading challenge," in [*MICCAI2009 workshop proceedings*], (2009).